
# Design and development of a thermal imaging system based on a temperature sensor array for temperature measurements of enclosed surfaces and its use at the body-seat interface

Zhuofu Liu, Le Chang, Zhongming Luo, Vincenzo Cascioli, Andrew I. Heusch, Peter W. McCarthy

PII: S0263-2241(17)30181-1
DOI: http://dx.doi.org/10.1016/j.measurement.2017.03.022
Reference: MEASUR 4659

To appear in: *Measurement*

Received Date: 10 December 2015
Revised Date: 4 March 2017
Accepted Date: 8 March 2017

Please cite this article as: Z. Liu, L. Chang, Z. Luo, V. Cascioli, A.I. Heusch, P.W. McCarthy, Design and development of a thermal imaging system based on a temperature sensor array for temperature measurements of enclosed surfaces and its use at the body-seat interface, *Measurement* (2017), doi: http://dx.doi.org/10.1016/j.measurement.2017.03.022

# Design and development of a thermal imaging system based on a temperature sensor array for temperature measurements of enclosed surfaces and its use at the body-seat interface

**Zhuofu Liu[1*], Le Chang[1], Zhongming Luo[1], Vincenzo Cascioli[2], Andrew I Heusch[3], Peter W McCarthy[3]**

[1] The higher educational key laboratory for Measuring & Control Technology and Instrumentations of Heilongjiang Province, Harbin University of Science and Technology, Harbin, Heilongjiang, 150080, China

[2] Murdoch University Chiropractic Clinic, Murdoch, 6150, Western Australia

[3] Welsh Institute of Chiropractic, University of South Wales, Treforest, Pontypridd, CF37 1DL, United Kingdom

Email address:

zhuofu_liu@hrbust.edu.cn (Z. Liu; [*]corresponding author),

1270828386@qq.com (C. Chang),

liuzoff@aliyun.com (Z. Luo),

V.Cascioli@murdoch.edu.au (V. Cascioli),

andrew.heusch@southwales.ac.uk (A. Heusch),

peter.mccarthy@southwales.ac.uk (P. McCarthy)

## 1 Introduction

Although there is recognition of the need for regular exercise, human beings appear to be progressively creating an environment that favours a sedentary lifestyle involving greater interaction with sitting and reliance on technology. Employees reportedly spend at least six hours a day seated, especially in professions such as banking, insurance, administration, call centres and transportation [1-3]. Many in such occupations tolerate the relative lack of activity and, as a consequence, risk developing one of the many diseases or disorders associated with this lifestyle. To compound this problem, many of these people also relax at home, spending prolonged sitting periods while either taking part in computer-based gaming, or simply watching television. As a result, ensuring provision of comfortable supporting seat surfaces to customers has become a major area for seat manufacturers who are keen to distinguish their products from other competitors [3].

In addition to the issue of comfort, it is important to consider the healthcare issues associated with prolonged sitting. For example, analysis of comfort or discomfort during short term sitting and a greater understanding of its relationship with potential tissue damage may be employed to develop smart seating to assist those with defective or absent sensory feedback (e.g., due to neural damage or even aging). This type of intervention may be able to put these people back in control and reduce their risk of skin damage and pressure sore development from prolonged periods of sitting.

Various evaluation approaches, both objective and subjective, have been utilised to investigate the negative effects of sedentary lifestyle on health [4-7]. Objective methodologies have attracted widespread attention from researchers [8-12], due to their generally having increased reliability, being generally less time consuming and less reliant upon large population study. They have also proved more efficient in the process of iterative seat design [5, 7]. Among these objective measurement parameters, body-seat interface temperature has played a pivotal role in the evaluation of comfort perceived by occupants [3, 7]. However, the studies conducted to explore this aspect of seating comfort or discomfort have so far been limited due to the difficulties of monitoring the thermal interaction between lower extremity and seating surface without either creating a local microclimate [8] or, disturbing the subject to make the measurement [3, 9].

Thermistor probes [7], sensors [9] and infrared thermography [8] have typically been used to

study thermal variations between the body and the seat surface, however, each has limitations. Due to the delicate nature of thermistor probes, they are typically deployed in the core of seat cushions [7] which results in measurement limitations related to insulative properties of the cushion material. Infrared imaging is able to map the temperature distribution over the entire surface of wheelchair cushions [8]; however, this is only possible when the subjects stand up (for 30 seconds every five minutes) to allow the assessment process to occur. Such intermittent measurement is not optimal as it could lead to cooling of the cushion surface as well as allowing physiological redistribution of blood, thus limiting the pooling effect of sitting. Furthermore, such an approach would also seriously limit any study of those who might benefit from a greater understanding of this modality (e.g. wheelchair bound subjects).

Over the past 10-15 years, the advancement of integrated circuit techniques has resulted in increased availability of Micro Electronic Mechanical System (MEMS) based temperature sensors. These small sensors are capable of addressing some of the above limitations of temperature measurement at the user-seat interface including placement under the seat cover on the cushion. We have previously demonstrated that it is possible to capture and analyse temperature information at various critical points of the user-seat interface [9, 12]. These experiments revealed that there was laterality to the temperature profile, with an unequal output from under each thigh; furthermore, the coccyx region also was shown to have a significantly different temperature from the thighs [9]. However, these studies were limited by the lack of precise placement, primarily the result of the limited coverage of the few sensors used: leading to our making assumptions in relation to temperatures across the seat surface [9]. Regardless of the aforementioned limitations however, we have more recently shown that reasonably accurate predictions can be derived from even this limited sensor number [13]. In order to acquire a more comprehensive, accurate and reliable information regarding the thermal profile between the body and the seat surface, it is essential to develop a more advanced temperature measurement system capable of more thoroughly monitoring the overall thermal distribution of the entire interface, such as those systems currently available for mapping pressure [10].

Among the different possibilities regarding mapping, there are commercially available products such as the FSA system (Vista Medical Ltd; Winnipeg, Manitoba, Canada). The FSA system has large sensor arrays (32 x 16) and is based on a matrix of interconnected piezoresistors [10]. Additional

conditioning circuits are necessary to coordinate such a large amount of piezoresistive sensors, resulting in issues related to both reliability and stability of the piezoresistive sensors when used in harsh environments [11]. Indeed, it is our experience that regular recalibration is advisable in order to ensure reliable measurements. As mentioned above, these sensors and their interlinked circuits can be affected by the environment (e.g., temperature) and the parameter they are measuring (pressure). Prolonged exposure to pressures can lead to creep in the output, furthermore, unloading or reduced loading during prolonged pressurisation is associated with hysteresis [10].

In this paper, we report a potential solution to reliable mapping at the seat surface and the body interface. The enhancements include replacement of the analog voltage output type of temperature sensors with digital output MEMS-based sensors, and expansion of the number of sensors from three to 64 by establishing an 8×8 sensor array / matrix. The aim was two-fold, to map a larger area and create a more reliable output which will enable the creation of an accurate understanding of the thermal distribution at this important interface. To visualise and analyse the collected data, we propose a sensor-array-based thermal “imaging” technique, which can not only continuously and more completely monitor the thermal variations between the lower extremity and the seat surface, but also has the capability to distinguish different sitting postures. Although the solution described here has applications to seating, there are many other situations where this approach can facilitate major increases in understanding of temperature (or other sensor-based parameters) changes in enclosed environments.

## 2 System descriptions

The developed system was constructed to incorporate the following features, as far as possible: unobtrusiveness, portability and ease of use. A further element was to allow for ease of replacement of the sensors used, in case of damage. Finally, and arguably the most important considerations of cost and accessibility of the data from the whole array by a single personal computer (PC) were the major motivation of the system development.

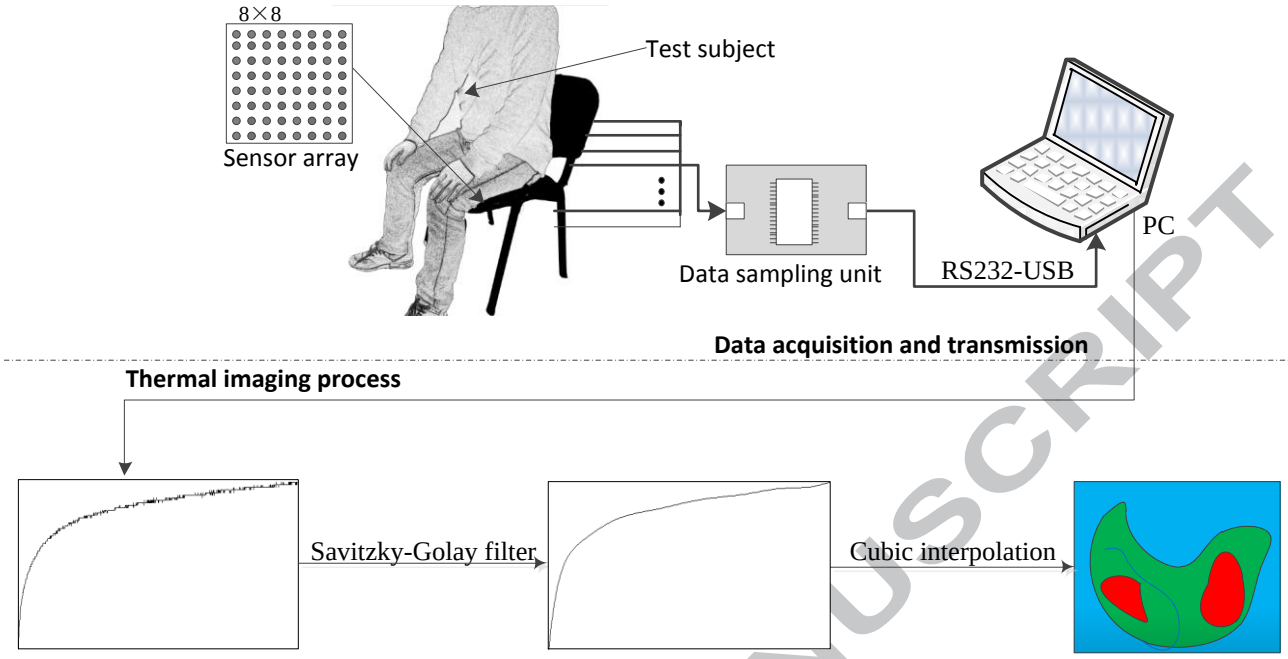


Figure 1 Composition of the measurement system based on the temperature sensor array. The system is able to convert the acquired body-seat interface temperature information into thermal matrix images.

By way of an overview, the system comprised three main parts: an array of temperature sensors, a data-sampling unit and a computer for data processing and analysis. The temperature sensor array served to convert temperature information to electric signals, while the data sampling unit acquired digital outputs from the sensors in the array and transmitted these to the computer for further analysis and conversion into temperature parameters for interpretation and calibration (Figure 1).

## 2.1 Design of temperature sensor array

A total of 64 MEMS sensors (DS18B20, Maxim Integrated, USA) were arranged on a seat surface with a separation of 48.0 ± 4.9 mm in the horizontal and 50.4 ± 5.0 mm in the vertical (Figure 2) between neighbouring sensors. The area covered was approximately 330 mm (horizontal dimension) × 385 mm (vertical dimension) = 127,050 $mm^2$. This arrangement of sensors significantly avoided mutual interference induced by the movement of the seated subjects in the process of data acquisition. Each sensor was individually sealed in a waterproof metallised plastic package that also prevented interference from static electricity. Owing to the arrangement and profile of the sensors, once the subjects had been seated on the array they did not appear to notice any significant difference with normal sitting and did not appear to alter the subjective perception of sitting comfort (informal feedback).


Figure 2 Photographic illustration of the proposed temperature measurement array placed on the surface of a test chair and the physical size of a DS18B20 temperature sensor sealed in a waterproof metallised plastic package.

Each temperature sensor had used 1-wire data transmission, therefore, it was not possible to assign all 64 sensors to an independent General Purpose Input Output (GPIO) microprocessors' port as each required a single digital port, which would exceed the total pin numbers of the selected microprocessor (STC15F2K60S2: Nantong Microelectronics Co., Jiangsu Province, China). This issue was solved by two modifications: firstly creating a custom-made electronic circuit which was used to connect all sensors to one GPIO port of the microprocessor and secondly identifying each sensor by its unique silicon serial number contained in the sensors' Read Only Memory (ROM) register. Such an approach is not suitable for traditional analog sensors which require independent Analog-to-Digital Converter (ADC) connections. The method described above also offers greater performance than the alternative of using auxiliary multiplexer chips along with GPIO ports.

The use of the serial number on the ROM as a unique address for each sensor gives the additional advantage of allowing for increases or decreases in the number of sensors used in any array. Consequently, the sensor array can be made to measure for the area over which any temperature measurement or mapping is required. Furthermore, the shape of the sensor array is not limited as it can be configured to different patterns and each sensor can be allocated to a position in that pattern. In addition, sensors can be replaced easily within the matrix and their unique ID can then be encoded to the position they have in the matrix. These advantages are the result of each sensors' independent connection to the microprocessor. Consequently, the mapping array can be formed in the shape of the seating area and not limited to being a square or rectangle; e.g., bicycle saddle shaped. This easy configuration allows it to be applied to different applications, while traditional devices or commercial products (FSA) only provide limited choices.

## 2.2 Realisation of the data acquisition unit

In order to meet the requirements of data acquisition and transmission, the STC15F2K60S2 (Nantong Microelectronics Co., Jiangsu Province, China) microprocessor was selected as its use would fulfil related tasks such as sensor initialisation, register management and data communication with the PC. This one-chip microprocessor has a selectable working frequency range from 4MHz to 35MHz and can execute programming codes at the speed up to 100 Million Instructions per Second (MIPS).

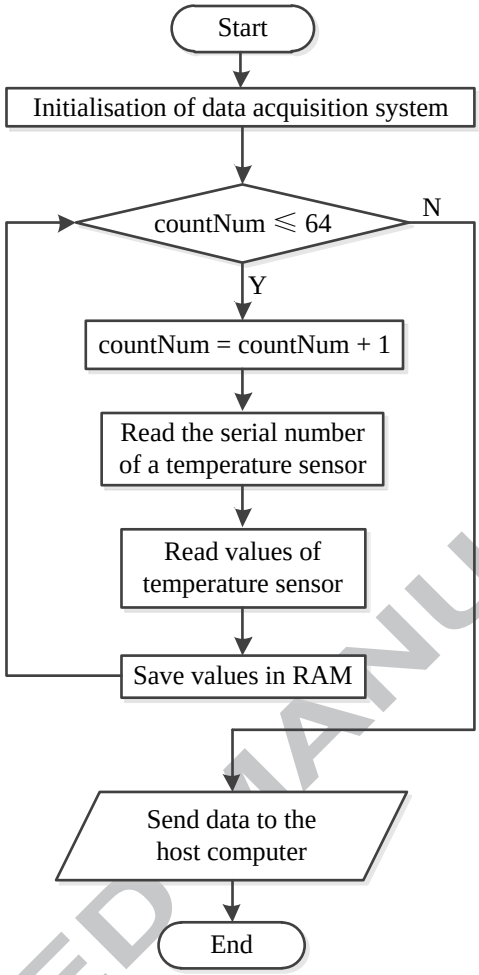


Figure 3 Program flowchart for the microprocessor. Up to a count of 64 the acquired data is stored in the microprocessor RAM, at count 65 the data being stored is communicated to the host computer. These steps are executed cyclically until the operator stops the process manually.

A working cycle of 11.0592MHz was chosen in order to ensure accurate data transmission. Furthermore, this type of one-chip microprocessor (STC15F2K60S2) is integrated with a 64K flash memory and 512 Bytes Random Access Memory (RAM) as there is a need for temporary data storage. The default sampling frequency of the system was set 30Hz/channel, as the previous experience suggested that temperature values would not be expected to change abruptly over very short periods (< 1 second) such as these. The data collected from all 64 sensors in a single pass were transmitted to the computer over a Universal Serial Bus (USB) interface with a baud rate of 9600 bps (bits per second). The conversion from the Universal Asynchronous Receiver Transmitter (UART) interface of the microprocessor to the USB interface of the computer was achieved with the help of a FT232R (Future Technology Devices International Ltd., UK) integrated chip. The operating strategy of the microprocessor can be seen in Figure 3.

A further advantage of this system over commercially available products such as the FSA, is that of cost. The prototype system described here comprised temperature sensors at approximately US$ 45 for the whole array and a custom-made data acquisition unit costing less than US$ 10.

### 2.3 Computer software development

A “user friendly” program was developed under the integrated development environment of Visual C++ (Microsoft Inc., U.S.A) in order to monitor the data acquisition process on the computer screen. This computer-based application software has the capability of simultaneously storing sampled data to the hard drive of the computer for further off-line analysis. The same program is capable of displaying the real-time trending curve of the body-seat interface temperature as well as adjusting system parameters (such as sampling frequency and recording duration) prior to the process of data collection. For further analysis, Matlab (MathWorks, USA) was employed (see below: Section 4).

## 3 System performance assessments

### 3.1 Evaluation of sensor array

In order to evaluate the performance of all 64 temperature sensors, they were placed in a traceably calibrated, standardised temperature chamber (PVS-3KP, ESPEC Environment Equipment Co. LTD., USA) capable of providing reliable temperatures from -20 ± 0.5 ℃ to 100 ± 0.5 ℃ (Certificate No: ISO 04308Q11746R0M and EN AC/0708030). A calibration range of 20 ℃ to 40 ℃ was selected to evaluate the performance of the sensors which encompassed the expected minimum and maximum temperature values found at the body-seat interface during a >15-minute sitting experiment [9]. The evaluation process started with a chamber temperature of 20 ℃, increasing in increments of 1 ℃ with readings from the sensors being recorded after the temperature of the chamber had reached a steady state (± 0.1 ℃ deviation from the pre-set values). An acquisition duration of 30 seconds was used at each testing point in order to avoid fluctuations. Averaged values for all 64 sensors at each specific temperature point were calculated using data sets derived from a 30-second recording period. The maximum standard deviation found for any of the 64 sensors was 0.3 ℃ : which was in agreement with the accuracy described in the manufacturers’ specifications presented in the sensors’ datasheet. In addition, on evaluating with an ascending temperature in the chamber, the sensors exhibited an approximate linear response in

comparison to the actual temperature setting for the chamber (see Figure 4).

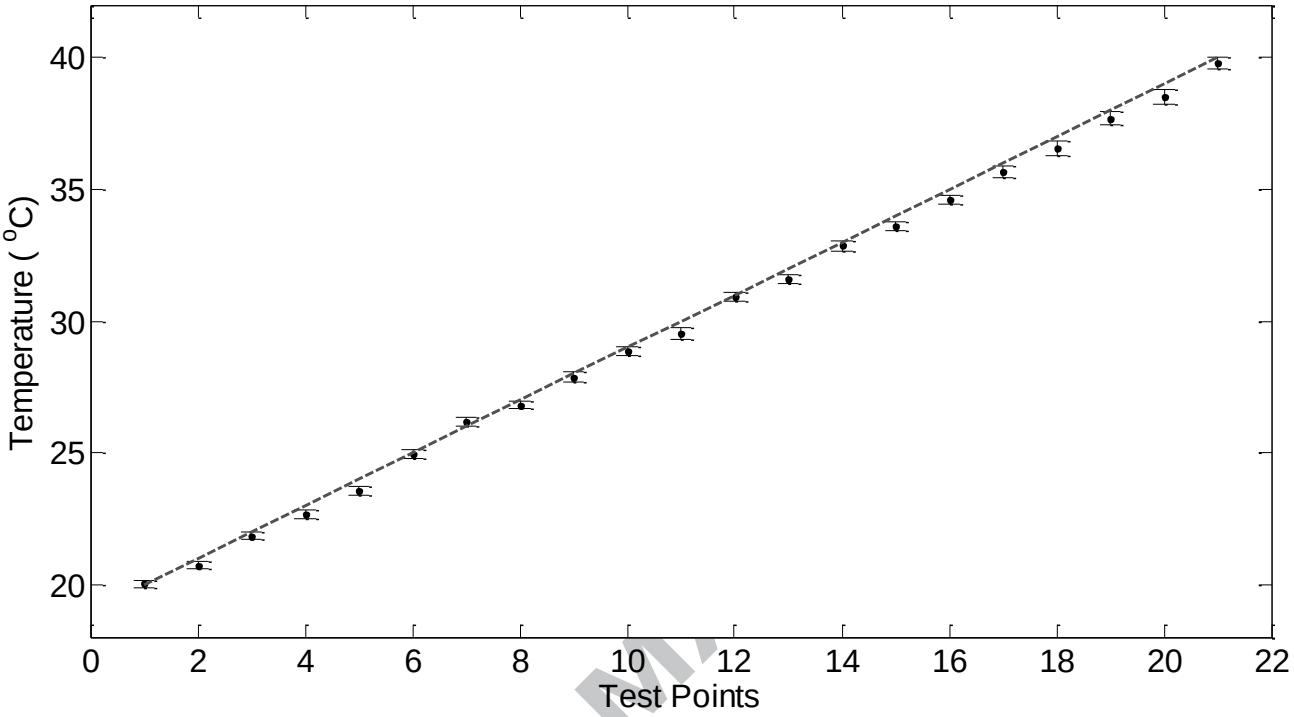


Figure 4 Statistical results of all 64 sensors in the process of performance evaluation. The black dots (•) represent the average values of the temperature sensors based on the 30-second recordings while the error boundaries correspond to the standard deviation at each test point. The expected value is indicated by the grey dash line (--) which is derived from the output of the temperature chamber.

## 3.2 Thermal radiation

All sensors were exposed to an open air environment in the research laboratory (average room temperature: 24.7 ± 0.3 ℃; average relative humidity: 44 % ± 3 % RH) in order to investigate any thermal emissions from either the temperature sensors or the circuitry while in use. The research room was vacated and sealed for the extent of the experiment to avoid introducing unnecessary variables and any additional uncontrolled external influences affecting the results. Infrared thermal emissions, either from the environment or the sensors, neighbouring circuits or their soldered joints during the period of operation, were monitored using a commercially available infrared camera (A615, FLIR Systems Inc., USA). Thermal images of the operating sensors mounted on the seat surface were taken every minute for one hour. Throughout this experiment, the temperature values (as determined from the infrared thermal emissions) for all 64 sensors varied between 24.4 ℃ and

24.7 ℃ (mean ± SD: 24.6 ± 0.1 ℃). The results confirmed that the temperature measurement system did not create any significant additional thermal emission.

## 4 Thermal imaging algorithms

### 4.1 Data pre-processing

Interference (noise) and voltage offset are major uncertainties that could affect the whole sensor array. Therefore, a Savitzky–Golay filter was applied to the original data in order to smooth the collected raw data. The Savitzky–Golay filter was chosen, over other alternatives, because it has the capability of increasing the signal-to-noise ratio without greatly distorting the signal [14-16]. The process was implemented with the help of a local convolution technique, which fitted successive sub-sets of adjacent data points with a local least-squares (LS) polynomial approximation as follows: suppose that for a sequence of sample points $x_n$ $(-M \le n \le M)$, the aim would be to fit a polynomial to the samples using the LS method, the polynomial could be defined as:

$$Q_n = \sum_{\mathrm{k}=0}^{\mathrm{p}} a_k n^k \tag{1}$$

Searching the polynomial coefficients (i.e., to resolve all optimal $a_k$ values in equation (1)) is equivalent to minimising the following cost function [14, 15]:

$$\boldsymbol{\mathcal{E}_p} = \sum_{n=-M}^{M} (Q_n - x_n)^2 = \sum_{n=-M}^{M} \left( \sum_{k=0}^{p} a_k n^k - x_n \right)^2 \tag{2}$$

According to the proof [14-16], the optimal polynomial coefficients can be obtained by differentiating $\boldsymbol{\mathcal{E}_p}$ with respect to each of the unknown coefficients and setting the corresponding derivative equal to zero:

$$\sum_{k=0}^{p} \left[ \left( \sum_{n=-M}^{M} n^{j+k} \right) a_k \right] = \sum_{n=-M}^{M} n^j x_n \qquad \mathrm{j} = 0,1,2 \ldots\ldots, \mathrm{p} \tag{3}$$

To simplify the procedure, the above equation can be written in the matrix form:

$$\mathbf{Ba} = \mathbf{A^T Aa} = \mathbf{A^T x} \tag{4}$$

where both, $\mathbf{a} = \left[a_0, a_1, \ldots\ldots, a_p\right]^{\mathrm{T}}$ and $\mathbf{x} = [x_{-M}, \ldots\ldots, x_{-1}, x_0, x_1, \ldots\ldots, x_M]^{\mathrm{T}}$ are vectors. The (2*M*+1) × (*p*+1) matrix **A** is called the design matrix for the polynomial approximation problem, with elements $\alpha_{n,j} = n^j;\ -M \le n \le M, j = 0,1,2, \ldots\ldots, p.$ The matrix $\mathbf{B} = \mathbf{A^T A}$ is a (*p*+1) × (*p*+1)

symmetric matrix with elements $\beta_{j,k} = \sum_{n=-M}^{M} n^{j+k}$; $j,k = 0,1,2,\ldots\ldots,p$. Therefore, the solution for the polynomial coefficients can be expressed as:

$$\mathbf{a} = (\mathbf{A^T A})^{-1}\mathbf{A^T x} = \mathbf{Hx} \quad (5)$$

Schafer showed the first row of the matrix **H** = $(\mathbf{A^T A})^{-1}\mathbf{A^T}$ represented the flipped impulse response coefficients of the Savitzky–Golay filter [14]. So, the coefficients of the Savitzky–Golay filter (the first row of the matrix **H**) can be obtained using efficient matrix inversion techniques [15, 16].

Offset removal was performed by initially calculating the average values of the initial readings for each of the 64 temperature sensors, then using each averaged value as a reference point for the corresponding channel [17]. The difference between the measurements made during the experiment and these references were used as input to form the thermal map. In another word, the thermal matrix map (image) was composed of measurements taking into account the small, but relevant, correction made to compensate for the initial offset between the sensors; hence the measurements reported should be directly comparative in terms of absolute temperature measurement.

## 4.2 Thermal matrix mapping

As the developed system collected data from 64 channels (eight columns by eight rows), it would be inconvenient to visualise the temperature information using a 1-dimensional curve under the usual time-amplitude coordinate system. Inspired by available infrared thermal imaging methods, the 1-dimensional temperature values of all 64 channels were converted into a 2-dimensional thermal matrix map. The final system was capable of recording temperature variations in real time (refreshing data for the whole array each 1/30 sec) without sacrificing measurement continuity, which is superior to a simple thermography-based seat temperature measurement system.

A cubic interpolation algorithm was employed in order to generate an image from the thermal matrix map [18]. To illustrate this, let (x,y) be a point in the rectangular subdivision $(x_m, x_{m+1}) \times (y_n, y_{n+1})$. The function of the cubic interpolation can then be written:

$$p(x,y) = \sum_{i=-1}^{2}\sum_{j=-1}^{2} a_{i+m,j+n}\mathcal{K}\left(\frac{x - x_{i+m}}{\Delta_x}\right)\mathcal{K}\left(\frac{y - y_{j+n}}{\Delta_y}\right) \quad (6)$$

where the coefficients $a_{i,j}$ are the pixel values for the interior grid points of $(x_i, y_j)$, otherwise they can be determined by the boundary conditions [18]. $\Delta_x$ and $\Delta_y$ are sampling steps in the x or y direction of the image coordinate system. The interpolation kernel function $\mathcal{K}$ can be defined as:

$$\mathcal{K}(a) = \begin{cases} \frac{3}{2}|a|^3 - \frac{5}{2}|a|^2 + 1 & 0 < |a| < 1 \\ \frac{-1}{2}|a|^3 + \frac{5}{2}|a|^2 - 4|a| + 2 & 1 < |a| < 2 \\ 0 & |a| > 2 \end{cases} \quad (7)$$

## 5 Results and discussion of *in situ* experiments

In order to demonstrate the effectiveness of the developed system, several *in situ* experiments were undertaken in the research laboratory. In the following trials, the subject reported being unaware of the presence of the temperature sensor array; which was an important confirmation since the primary purpose of this development was to provide a comfortable, discrete and unobtrusive measurement system that would not change the behaviour of those being observed.

### 5.1 Temperature variations over the entire body-seat interface

Temperature mapping was performed with a subject sitting on a commercially available chair mounted with the temperature sensor array (seen in Figure 2) for 20 minutes. Based on our previous studies [9, 12, 13], such a recording method could be used to gather thermal information from the body–seat interface without having an adverse effect on their seating comfort. Both the ambient temperature and its relative humidity of the laboratory were monitored during the experimental period and remained relatively stable (25.2 ± 0.3 ℃; 45 % ± 4 % RH, respectively).

The sequential thermal images presented in Figure 5 illustrate the temprature profile across the entire seating surface. Importantly, they can be used to indicate where the highest temperatures were being created. In the experiment, temperature increased mostly under both thighs (up to 7.0 ℃) followed by the ischial tuberosities (up to 6.1 ℃). This finding is consistent with previously published results based on use of an infrared camera [8]. However, as mentioned above, thermography-based techniques fail to offer continuously monitoring of thermal information at the body-seat interface, disturbing the interface with the periodic interruptions required for capturing thermograms. The information produced by the system descibed here is more likely to accurately represent the magnitude of the thermal changes, simply because the data were gathered

continually without the need to disturb the interface region being studied. The system also allows for a more accurate and reliable identification of peak temperature regions (such as thighs and ischial tuberosities) than other systems that record continually from the interface region. Combining these advantages might prove instrumental in ensuring more efficient monitoring and thus care of those confined to long-term sitting in wheelchairs.

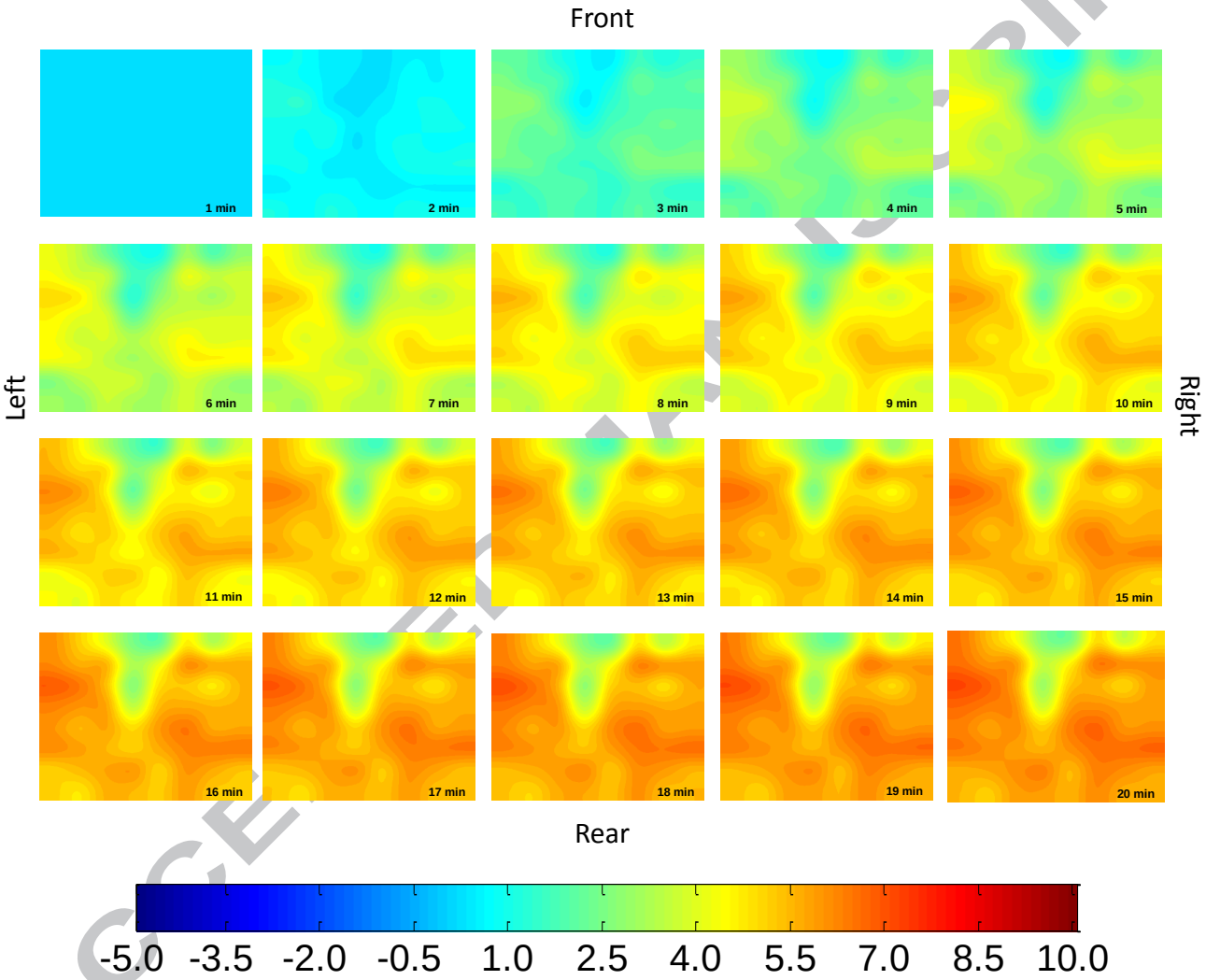


Figure 5 A photomontage of sequential temperature maps (taken every 60 seconds) during a 20-minute experiment where a subject sat quietly on a commercially available chair. Each image is aligned to show the front of the seat at the top, the rear at the lower edge and left / right sides as indicated. The initial map (the top left image) shows little variations in temperature, whereas the final image (the bottom right image) taken at the 20$^{th}$ minute shows distinctive variations in temperature. Thermal maps represent the distribution of changes in temperature over the entire surface, as calculated using the difference from the corrected initial temperature reading (see text above 4.2 for detail). Below the final series of thermal images the temperature calibration reference bar can be found which relates the difference in temperatures (℃) from the initial reading to the pseudo-colour images in the Hue Saturation Value (HSV) colour model.

The above information may be of use to caregivers for those who sit for long periods and do not have the capability to recognise when they need to move. This system can more easily and efficiently recognise the temperature cues which would suggest the need to alter the position of wheelchair-bound or bed-ridden individuals in order to reduce their susceptibility to ulcer formation or endothelial cell compromise in superficial femoral artery damage [19]. Furthermore, this capacity to ensure continous measurement has overcome the impracticality of both thermography-based temperature detection which required repeated standing in the process of data acquisition, especially for disabled patients, and systems involving limited number of temperature sensors, where movement might easily lead to the sensor being in the wrong position in relation to the "hot spot". As a result, the information obtained by the system reported here should be sufficiently reliable to be applied in clinical situations and might therefore see a future role in therapeutic monitoring in order to reduce the likelihood of the problems outlined above.

Another interesting finding was that the temperature distribution revealed by the sensor array did not exhibit in a symetrical fashion over the body-seat contact surface (Figure 5). For example, the peak temperature value was 7.0 ℃ under the left thigh region while the maximum value was 6.6 ℃ under the right thigh. This discovery inspired us to perform further pilot trials to explore the relationship between the temperature distribution and different sitting postures, which will be addressed in the following section.

## 5.2 Thermal map for different sitting postures

In order to initiate an investigation into the effect that different sitting postures may have on thermal distribution, a single subject was used. The subject wore jeans and was asked to perform four independent trials by sitting on the aforementioned chair in each of four relatively common seating positions (sitting-up straight, leaning-backward, sitting crossed legged, with either his left leg on the right thigh or right leg on the left thigh). The duration of each trial was 20 minutes, since changes in temperature during sitting have been shown previously to approximate a plateau by the end of that period [9]. After each trial, the test chair with the embedded temperature sensor array was left to re-equilibriate with the environmental ambient temperature (usually half an hour) before the next experiment was initiated. The average room temperature was 25.1 ± 0.3 ℃ and the average relative humidity was 43 % ± 2 % RH during the process of the four trials. The thermal maps

revealed obviously discriminating characteristics over the entire surface corresponding to each sitting posture, as can be seen in Figure 6.

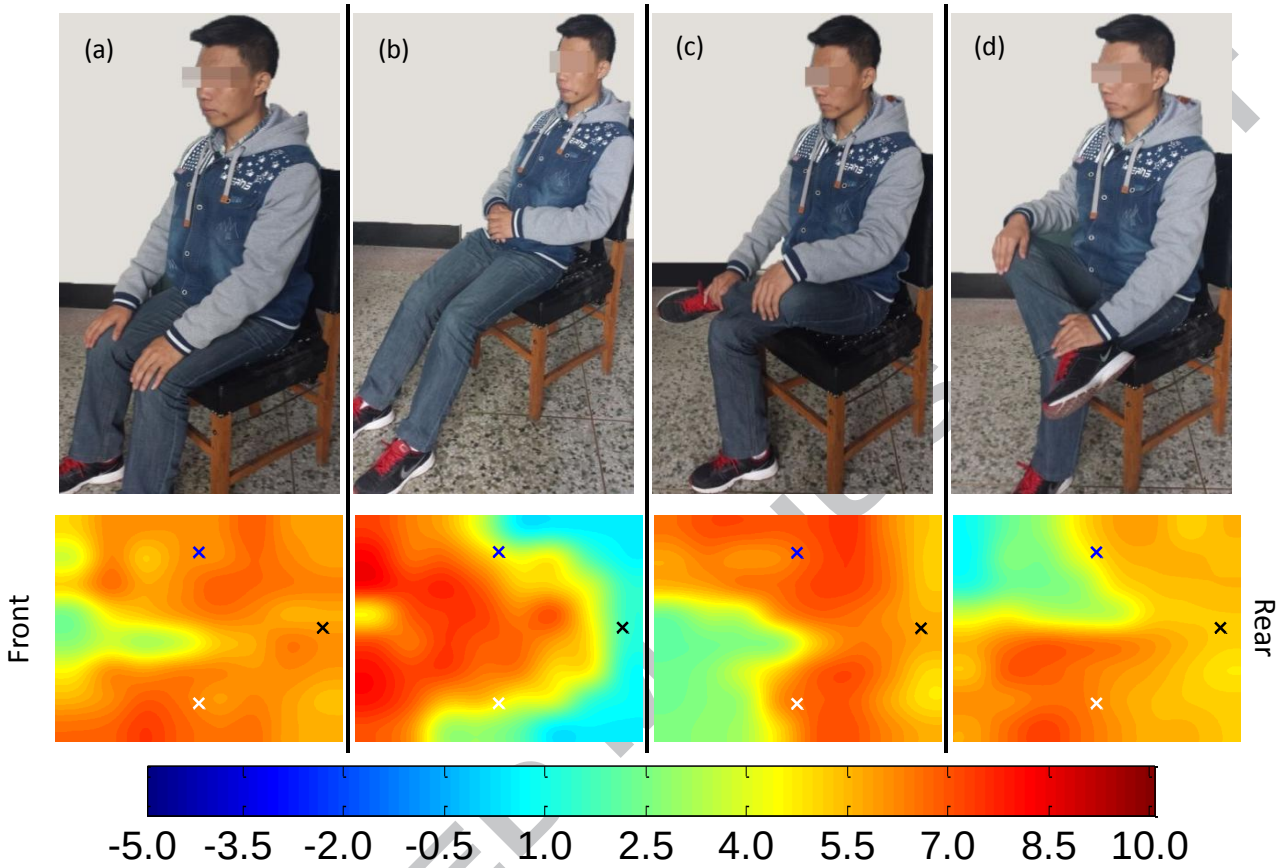


Figure 6 Data from four different sitting postures using data from the 20th minute (final) image only. Images from left to right depict results of four commonly sitting postures (a: sitting-upright, b: leaning-backwards, c: left leg on the right thigh and d: right leg on the left thigh). The top photographs show the seated postures which produced the thermal images below them. The thermal images have been aligned with the rear of the seat at the right hand side of the image and the front at the left hand edge. To give a better comparison between the newly designed system and previously reported system, the three sites used as measuring points in those experiments were superimposed on the thermal images. The white and blue "X" markers represent left and right mid-thigh respectively, with the coccyx measurement point being indicated by a black "X". Thermal maps represent distribution of changes in temperature over the entire surface, as calculated using the difference from corrected initial temperature reading from each sensor (see text for detail). The calibration reference bar can be found below the thermal maps: please note the pseudo-colour in the images in the HSV colour model numbers relates to the difference in temperature (°C) from the initial reading.

The advantages of thermal mapping and the images derived from the sensor array output are apparent when compared to the traditional temperature measurements based on a limited number of thermistor probes (Figure 6). Primarily, the thermal mapping overcomes the inherent

drawbacks of recording data from limited regions around the sensors (markers superimposed on the thermal images in Figure 6). Additionally, there is the ability to study the distribution of temperature and locate the hottest region, as a result of having more comprehensive information, e.g. sitting patterns can be acquired from the thermal map. Furthermore, the thermal map offers the opportunity to examine how sitting postures can be related to temperature distribution over the entire skin contact with the seat surface. This type of capability has been presented for body and seat interface pressure determination for many years, with interface pressures being commonly studied with the help of pressure mats. However, over the past decades there has been a growing awareness of the importance that factors other than pressure have in relation to epidemal and vascular damage as well as eventual skin ulceration [6-8]. Therefore, the approach proposed by this research should offer the opportunity for both scientific and clinical usage to derive greater insight into the relationship between temperature (and any other property measureable by sensors) and factors such as skin damage and percieved comfort when sitting or lying down for prolonged periods.

## 5 Conclusions

In this paper, a novel body-seat interface temperature measurement system was presented based on an array of 64 MEMS-based temperature sensors. The advantages of the system included: 1) continuously monitoring of temperature changes between the seat surface and the skin, 2) provision of a map revealing the temperature distribution over the entire contact surface, 3) identification of changes in different seating styles from the detail provided in the thermal images. The potential use of this system covers both scientific study, clinical monitoring and alerting systems to facilitate healthcare of the chronic wheelchair-bound person with the aim of preventing ulcer or other associated skin or vascular damage.

## Acknowledgements

This work was supported by Natural Science Foundation of Heilongjiang Province (Grant No. F201421), Harbin Scientific Innovation Project for Elite Young Researcher (Grant No. 2013RFQXJ093), and Scientific Research and Talent Project of Education Department of Heilongjiang Province (Grant No.12541109, 12541140).

## References

[1] W. Xu, M. Huang, N. Amini, L. He, M. Sarrafzadeh, eCushion: a textile pressure sensor array design and calibration for sitting posture analysis, IEEE Sensors Journal. 2013, 13(10): 3926-3934

[2] M. Elisa, B. Gian, C. Andrea, Design and development of a monitoring system for the interface pressure measurement of seated people, IEEE Transactions on Instrumentation and Measurement. 2013, 62(3): 570-577

[3] K. Anil, F. Tycho, B. Steven, Using a psychophysical approach to identify a user's self selected thermal comfort on a task chair, International Journal of Industrial Ergonomics. 2015, 46 : 36-43

[4] E. Pinheiro, O. Postolache, P. Girao, Empirical mode decomposition and principal component analysis implementation in processing non-invasive cardiovascular signals, Measurement. 2012, 45(2): 175-181

[5] L. Peter, R. Joseph, K. Gregory, M. William, Objective classification of vehicle seat discomfort, Ergonomics. 2014, 57(4): 536–544

[6] Z. Roland, T. William, L. Silvio. Are pressure measurements effective in the assessment of office chair comfort/discomfort? a review, Applied Ergonomics , 2015, 48: 273-282

[7] L. Stockton, S. Rithalia, Pressure-reducing cushions: perceptions of comfort from the wheelchair users' perspective using interface pressure, temperature and humidity measurements, Journal of Tissue Viability. 2009, 18(2):28-35

[8] M. Ferrarin, N. Ludwig, Analysis of thermal properties of wheelchair cushions with thermography, Medical & Biological Engineering & Computing. 2000, 38:31-34.

[9] Z. Liu, V. Cascioli, A. Heusch, P. McCarthy. Studying thermal characteristics of seating materials by recording temperature from 3 positions at the seat-subject interface, Journal of Tissue Viability. 2011, 20(3): 73-80.

[10] L. Pipkin, S. Sprigle. Effect of model design, cushion construction, and interface pressure mats on interface pressure and immersion, Journal of Rehabilitation Research & Development. 2008, 45(4): 875-882.

[11] S. Kim, K. D. Wise. Temperature sensitivity in silicon piezoresistive pressure transducers, IEEE Transactions on Electron Devices. 1983, 30 (7): 802 – 810.

[12] P. McCarthy, Z. Liu, A. Heusch, V. Cascioli, Assessment of humidity and temperature sensors and their application to seating, Journal of Medical Engineering and Technology. 2009, 33: 449 –453.

[13] Z. Liu, L. Wang, Z. Luo, A. Heusch, V. Cascioli, P. McCarthy, Microenvironment temperature

prediction between body and seat interface using autoregressive data-driven model, Journal of Tissue Viability. 2015, 24(4): 131-139

[14] R. Schafer, What is a Savitzky-Golay filter? IEEE Signal Processing Magazine, 2011, (28)4: 111-117.

[15] K. Sunder, S. Chandra, On the selection of optimum Savitzky-Golay filters, IEEE Transactions on Signal Processing. 2013, 61(2): 380-391

[16] K. Sunder, D. Mathew, S. Chandra, A Savitzky-Golay filtering perspective of dynamic feature computation, IEEE Signal Processing Letters. 2013, 20(3): 281 -284

[17] Y. Nam, P. Jung, Child activity recognition based on cooperative fusion model of a triaxial accelerometer and a barometric pressure sensor, IEEE Journal of Biomedical and Health Informatics. 2013, 17(2): 420-426

[18] R. Keys, Cubic convolution interpolation for digital image processing, IEEE Transactions on Acoustics, Speech, and Signal Processing. 1981, 29 (6): 1153-1160

[19] S. Thosar, S. Bielko, K. Mather, J. Johnston, J. Wallace, Effect of prolonged sitting and breaks in sitting time on endothelial function, Medicine and Science in Sports and Exercise. 2015, 47(4):843-849